Using Digital Image Correlation to Quantify Skin Deformation with Von Frey Monofilaments

Anika R. Kao, *Student Member, IEEE*, Chang Xu, *Student Member, IEEE*, and Gregory J. Gerling, *Senior Member, IEEE*

***Abstract*—Thin von Frey monofilaments are a clinical tool used worldwide to assess touch deficits. One's ability to perceive touch with low-force monofilaments (0.008 – 0.07 g) establishes an absolute threshold and thereby the extent of impairment. While individual monofilaments bend at defined forces, there are no empirical measurements of the skin surface's response. In this work, we measure skin surface deformation at light-touch perceptual limits, by adopting an imaging approach using 3D digital image correlation (DIC). Generating point cloud data from three cameras surveilling the index finger pad, we reassemble and stitch together multiple 3D surfaces. Then, in response to each monofilament's indentation over time, we quantify strain across the skin surface, radial deformation emanating from the contact point, penetration depth into the surface, and area between 2D cross-sections. The results show that the monofilaments create distinct states of skin deformation, which align closely with just noticeable percepts at absolute detection and discrimination thresholds, even amidst variance between individuals and trials. In particular, the resolution of the DIC imaging approach captures sufficient differences in skin deformation at threshold, offering promise in understanding the skin's role in perception.**

***Index Terms*—Touch, perception, skin deformation, DIC.**

I. Introduction

Damage to the nervous system can diminish tactile acuity. In particular, neuropathic conditions of allodynia and hyperalgesia can cause pain and sensory impairment as a result of traumatic injury, diabetes, vascular problems, or infection. To assess the extent of sensory impairment, clinicians commonly examine regions of a patient's skin by touch using thin monofilaments, designed to be portable and inexpensive. For example, von Frey and Semmes-Weinstein monofilaments have been used for decades [1], [2]. Each of about twenty monofilaments is constructed with a characteristic length, thickness, and material modulus in order to visibly buckle at a precise force upon indentation. Monofilaments in the range of 0.008 – 0.07 g indicate normal light touch near the absolute threshold of perception [1], while those in ranges of 0.16 – 0.4 g and 0.6 – 2.0 g point to diminished light touch and diminished protective sensation, respectively.

While individual monofilaments bend at defined forces, there have been no empirical measurements reported of the skin surface's response. Indeed, as the point of origin for encoding touch information, the skin's surface is where patterns of stress and strain are established, before propagating through the skin's layers toward end organs of mechanosensitive afferents [3]. Predicting the flow of such patterns can be complex because the skin is a composite structure, as opposed to a homogenous continuum, and varies substantially between body sites, persons, and genders. Ultimately, our perceptions of tactile acuity are shaped by some combination of factors involving the skin, afferents (subtypes, locations, morphologies, and densities), and various elements of the central nervous system. In effort to decouple those factors driving and limiting tactile acuity, therefore, we might first ask – how does the skin move?

Many empirical imaging approaches are emerging to capture 3D contour and deformation patterns of skin in response to moving stimuli. For example, the contact and movement of finger pad skin against rigid glass plates has been used to study slip [4], [5], and other efforts have considered elastic contact interactions [6]. While some approaches capture 3D surfaces at points in time, they often do not track specific regions of the skin over time, which is necessary to attain mechanical quantities of stretch and strain. To address this issue, digital image correlation (DIC) offers a way to match local pixel patterns from multiple camera angles to produce displacement and strain, where stitching multiple 3D surfaces together can avoid stimulus occlusion. DIC has been employed with skin [7]–[10], though mostly as limited to situations of lateral stretch. Optical coherence tomography (OCT) can offer even finer resolution and image a couple millimeters under the skin's surface, though it yields only single cross-sections rather than 3D surface geometry.

Here, we study how mechanical states of deformation at the skin surface, in response to indentation by von Frey monofilaments, drive just noticeable percepts at absolute detection and discrimination thresholds. In adopting a DIC imaging approach using standard high-resolution cameras, we seek to determine if its resolution and range are sufficient to capture differences in skin deformation at perceptual thresholds. Such capabilities offer promise in understanding physiological mechanisms underlying sensory impairments, and clinical implications of von Frey monofilaments.

II. Methods

This work adopts a DIC imaging approach to measure skin surface deformation at the finger pad upon indentation by von Frey monofilaments of various bend forces. From point cloud data generated from three cameras surveilling the index finger pad, we reassemble and stitch together 3D surfaces. Per monofilament, we quantify strain across the skin surface, radial deformation emanating from the contact point, penetration depth into the surface, and area between 2D cross-sections. Psychophysical experiments evaluate absolute detection and discrimination thresholds.

This work was supported in part by the National Science Foundation (IIS-1908115, NRT-1829004) and National Institutes of Health (NINDS R01NS105241).

The authors are with the School of Engineering and Applied Science, University of Virginia, Charlottesville, VA 22904 USA. The corresponding author is G. J. Gerling (phone: 434-924-0533; e-mail: gg7h@virginia.edu).

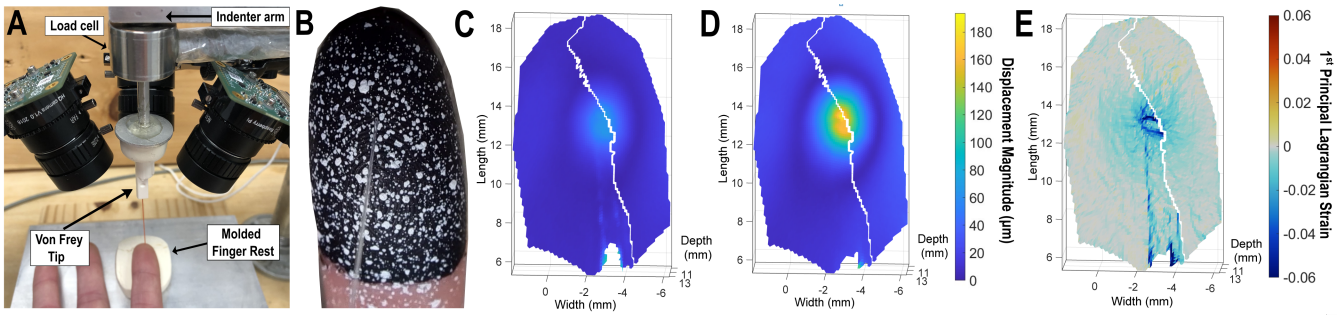

Figure 1. Experimental apparatus. (A) Indenter with load cell and von Frey monofilament attached. Three cameras around the indenter synchronously capture images for surface reconstruction via digital image correlation (DIC). (B) A von Frey monofilament (clear, buckles at force of 1 g/9.8 mN) makes contact with a speckled index finger. Randomly applied speckles (white) applied over base layer (black) create a unique pixel pattern to enable surface tracking. (C) – (D) Resultant 3D DIC tracking of skin deformation while in contact with monofilament, where point cloud shows displacement magnitude early (67 ms) and later (767 ms) into the indentation. Jagged white lines show where two overlapping 3D surfaces are stitched together. (E) First principal Lagrangian strain (767 ms). Blue color indicates negative strain, under compression, and yellow color indicates positive strain, under tension.

A. Experimental setup

The experimental setup in Fig. 1A and Video 1 was used for mechanical indentation of monofilaments and optical tracking of skin surface deformation at the index finger pad. Monofilament tips were inserted into a custom adapter, made from a metal plate and solid modeling clay, fitted to the cantilever of a vertical indenter, described previously [11]. The participant's index finger rested in a solid clay mold secured to a plate on the table, at 0 degrees. To capture optical data, an array of cameras was setup in a stereo configuration. Three monocular cameras (12 MP, Raspberry Pi High Quality, England) were connected to microcontrollers (Raspberry Pi Zero W boards, England), mounted to wide angle lenses (6 mm Vilros, Lakewood, NJ, USA), and fastened to vertical poles via a ball socket clamp.

B. von Frey monofilaments

The right index finger pad was indented with von Frey monofilaments (Touch Test Monofilaments – based on the Semmes Weinstein set, North Coast Medical Inc., Morgan Hill, CA, USA) ranging from 0.02 to 4.0 g. The monofilaments are made of nylon and vary in length, thickness, and material modulus, and are calibrated to visually buckle at a prescribed force [1]. Fig. 2 shows the indentation and buckling of a 1.0 g monofilament.

C. Paint speckling of finger pad skin

In using DIC, attaining a high spatial resolution of displacement fields depends on the size and size consistency of applied paint speckles, the density and randomness of their pattern, and a high foreground to background contrast ratio with equal amounts of light and dark on the specimen surface. To meet these conditions, participants' right index fingers were first covered with a layer of black, washable (non-toxic) acrylic paint (Craft Smart, Michaels Stores, Irving, TX, USA), to provide a consistent background. To create a high contrast foreground, white aerosol paint (Krylon, Sherwin-Williams Co, Cleveland, OH, USA) was sprayed onto bristles of a stiff paintbrush. While still wet, the bristles were swiped back and released to ricochet paint speckles onto the skin. This process was repeated to achieve the desired speckle density and contrast ratio. The paint dried within 60 s. The speckle sizes ranged in diameter from 0.1 to 1.0 mm, Figs. 1B and 2. After the experiments concluded, the paint was removed by soap and water.

D. Participants

Five healthy individuals (2 male, 3 female, 24 ± 2.6 years of age, mean ± SD) participated in the study. All participants reported being right hand dominant. All provided written informed consent for the study, which was approved by the local institutional review board. The devices and surfaces were sanitized, and all participants wore facemasks, following COVID-19 protocols.

E. Experimental procedures

Four experiments were conducted per participant, at a duration of two hours per participant. First, psychophysical absolute detection thresholds were evaluated using the monofilaments. Second, psychophysical discrimination thresholds were evaluated using three monofilament pairs. Third, biomechanical measurements of skin surface deformation to monofilament indentation were performed using DIC. We utilized the index finger pad of participants' right hand, with monofilaments indented perpendicular to the skin surface, a curtain to eliminate visual cues, and no feedback provided on their performance.

Absolute detection threshold: Following published protocols, eight von Frey monofilaments (0.02, 0.04, 0.07, 0.4, 1.0, 1.4, 2.0, 4.0 g) were indented sequentially in order of descending force, and then ascending force, for a total of 16 trials per participant [2], [12]. In each of the 16 trials, the participant was informed verbally of the start and stop time between the delivery of a series of 5 to 8 indentations. The number of indentations delivered per trial was selected randomly and conducted over 20 s. The indentations were manually delivered by the experimenter, as done clinically,

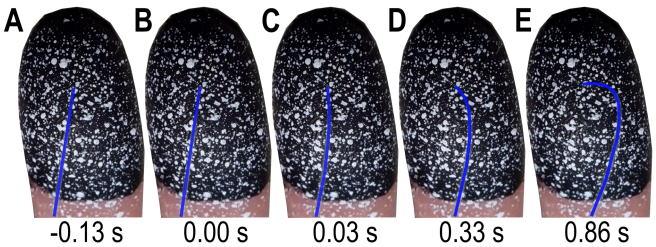

Figure 2. Buckling of 1.0 g von Frey monofilament. (A) Start of indenter motion before skin contact. (B) Contact with skin surface. (C) Start of monofilament buckle. (D) Increased buckling. (E) Maximum buckle. Note the monofilament was digitally enhanced to blue to make it more visible.

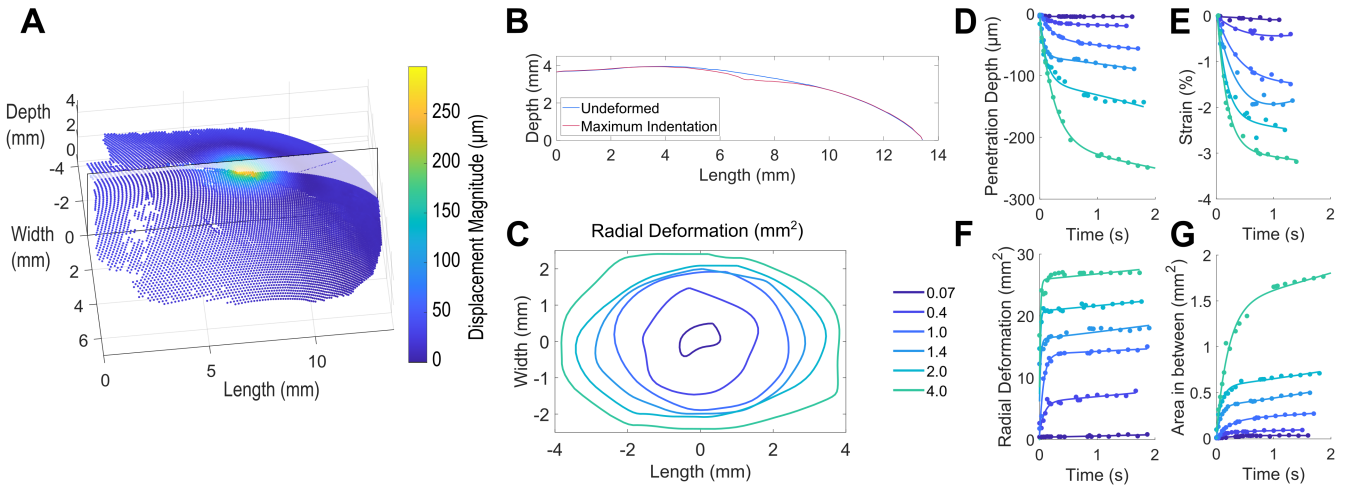

Figure 3. 3D skin surface deformation quantified to generate four derived metrics. (A) 3D point cloud showing displacement magnitude at maximum indentation in response to a 1.4 g von Frey monofilament. A cross-sectional plane is overlaid on the 3D point cloud, extending from proximal to distal fingertip. (B) The undeformed cross-section before contact and at maximum indentation. (C) Boundaries of radial deformation at maximum indentation for monofilaments between 0.07 - 4.0 g. (D) – (G) Four derived metrics, where plots show raw data (points) from one measurement trial with one participant fit by an exponential function. In particular, clear separation is observable between monofilaments, across all four derived metrics, as defined in Section II.G.

with a 1 s gap between indentations [13]. At the conclusion of each trial, the participant was asked to report the number of indentations. Approximately 20 s elapsed between trials. The threshold was defined as the monofilament above where the participant correctly perceived at least 80% of the 5 to 8 indentations in both descending and ascending order [12].

Discrimination threshold: Discrimination of von Frey monofilaments is atypical with their use in the clinic. However, for the purposes of comparing skin surface deformation and perceptual response, we evaluated three pairs (0.07, 0.4 g; 0.4, 1.0 g; 1.4, 2.0 g) thought to lie near discrimination thresholds, while spanning force magnitudes. Following the experimental design of a prior same-different procedure [14], each monofilament pair was tested in 8 trials where the order of the 3 stimulus pairs was randomized, for a total of 24 trials per participant. Within each trial, there was a 1 s gap between the first and second indentation. After the second indentation, the participant was asked whether the stimulus pair were the same or different.

Biomechanical measurement of skin contact: Six von Frey monofilaments (0.07, 0.4, 1.0, 1.4, 2.0, 4.0 g) were used to measure skin surface deformation. Prior to each indentation, the mechanical indenter positioned the tip of a monofilament 1 mm above the skin surface. Indentations were done in a displacement-control mode [6] and a preliminary indentation was conducted to determine the terminal displacement required to reach that monofilament's buckling force. Each was indented at 4 mm/s [15], held at terminal displacement for 2 s [13] and retracted at 4 mm/s. An example procedure is shown in Fig. 2 where a 1.0 g monofilament is held at rest, makes contact with the skin, and buckles at its calibrated force.

Effects of paint on absolute threshold perception: To consider possible perceptual effects of applying the paint layer to the skin, participants completed the same absolute detection task with and without paint. These conditions were evaluated on separate days with condition order randomized.

F. Imaging approach using digital image correlation

DIC is a non-contact, optical tracking technique that matches pixel patterns from multiple stereo camera angles to produce displacement and strain fields. It allows for multiple 3D surfaces to be stitched together to avoid occlusions and thereby accommodate highly curved surfaces. DIC uses cross-correlation of stereo-calibrated camera sets to measure movement of unique pixel patterns across frames. While one camera can track 2D images, a calibrated pair of cameras can correlate 2D information to produce 3D representations. Moreover, surfaces from multiple camera pairs can be merged into a cohesive surface of maximum correlation. We used open-source software MultiDIC [16], built atop Ncorr [17], to capture 3D skin surface deformation, strain fields, lateral stretch and motion.

To reconstruct 3D surfaces from 2D image frames, a stereo camera calibration step, to determine each camera's field of view and ensure overlap, is required before data collection. Video from each of the three cameras was captured synchronously at 30 frames per second and 1920 by 1080 pixels resolution (~25 to 30 pixels/mm) and compressed into the H.264 video format. To reduce time in processing the data, videos were converted back into images and select frames were chosen. About 20 frames were selected based on contact, buckle, and hold points as determined visually per trial. Two 2D surfaces per trial were processed, followed by a 3D surface stitching and reconstruction step, and a post-processing step. Each trial required about 3-5 hours of processing, for a total of 90 hours per participant.

Raw images in grayscale were input into the DIC software for computation. Two separate surfaces ([camera 1, camera 2], [camera 2, camera 3]), were stitched into a single surface to eliminate occlusion from the monofilament. Based on the diameter of paint speckles on the skin and the size of surface deformation given a monofilament, the subset radius was set to 15 pixels and spacing to 3 pixels to optimize feature tracking and data resolution [16].

G. DIC data analysis and skin deformation metrics

As shown in Figs. 1C-E and 3A, we generated 3D point clouds of mechanical quantities that include displacement magnitude and first principal Lagrangian strain. In particular, in Fig. 3A we show displacement magnitude at the terminal indentation for a 1.4 g monofilament. The displacement magnitude of the skin surface given the indentation of a monofilament is captured at select points of time at frames of contact, buckle, and in between.

Following the DIC analysis, to further quantify the deformation at the skin surface, we defined four derived skin deformation metrics, including penetration depth into the surface, strain across the skin surface, radial deformation emanating from the contact point, and area between 2D cross-sections (Figs. 3D-G). These metrics consider the extent to which the skin is both stretched laterally and indented normally, calculated from the initial contact frame through the buckle frame, to visualize changes in skin deformation up to that monofilament's calibrated force.

Penetration depth: In contrast to displacement magnitude, penetration depth is defined as the maximum displacement in the depth dimension, of a single point in the point cloud, from the undeformed (t = 0 s) surface. A representative trial for one participant in Fig. 3D illustrates clear differences between the monofilaments. To avoid noise, due to lighting, speckle variation, and other factors, penetration depth is plotted, following convention [18], as the 95th percentile of all data points per image frame, trial, and participant.

Strain: Strain is defined as the change, from the undeformed state, of first principal Lagrangian strain in compression over the skin surface. As it is typically more impacted by noise than penetration depth, strain is plotted as the 90th percentile of data points. Full-field strain is illustrated in Fig. 1E and the progression of strain over the time course of the indentation is illustrated in Fig. 3E.

Radial deformation: From the 3D point cloud (Fig. 3A), the field of points displacing more than 10 µm were fitted with a 2D ellipse [11]. Radial deformation is the area of this ellipse. As the monofilament indents further into the skin surface, more points begin to emanate radially from the point of contact, and thereby pass the threshold. Figures 3C, F show radial deformation ranging from 0.8 to 31 mm^2, increasing from initial contact and plateau until the calibrated force, at which point the monofilament bends, and little further deformation of the skin is observed.

Area between 2D cross-sections: Relating lateral deformation and penetration depth, the difference between the 2D cross-sections of deformed and undeformed surfaces was integrated to produce area. This was done along a plane in the depth-direction at the point of maximum displacement, extending proximal to distal (Fig. 3B).

To further analyze differences between monofilament pairs, integral differences for all deformation metrics were calculated, per pair used in the discrimination experiment, at a step size of 0.05 s. To normalize, each integral difference was divided by the average metric magnitude of the smaller monofilament over time, and multiplied by 100, yielding a percentage difference.

III. Results

A. Biomechanical measurement of skin deformation

Clear separation across all four skin deformation metrics is observed between all six monofilaments (0.07 – 4.0 g), outside of their 95% confidence intervals even amidst variance between individuals and trials (Figs. 4A-D). Across metrics and monofilaments, the data ramp upward upon initial skin contact within 0.5 s, and subsequently reach a plateau at the calibrated force at 0.5 to 1.5 s. The imaging method produces range and resolution such that penetration depth ranges from 6.1 – 248.9 µm, with non-overlapping 95% confidence intervals (Figs. 4A, E). Similarly, low strain values measured up to about 5% maintain separation and order across stimuli (comparable to [7]) with observed values as small as 0.34% (Figs. 4B, F). The radial deformation ranges from 0.96 – 25.90 mm^2 (Figs. 4C, G) while area between 2D cross-sections capture changes in surface curvature as small as 0.03 – 1.63 mm^2 (Figs. 4D, H).

B. Psychophysical evaluation of absolute detection and discrimination thresholds

With respect to absolute detection (Fig. 5A), the force threshold – set at 80% correct due to the experimental

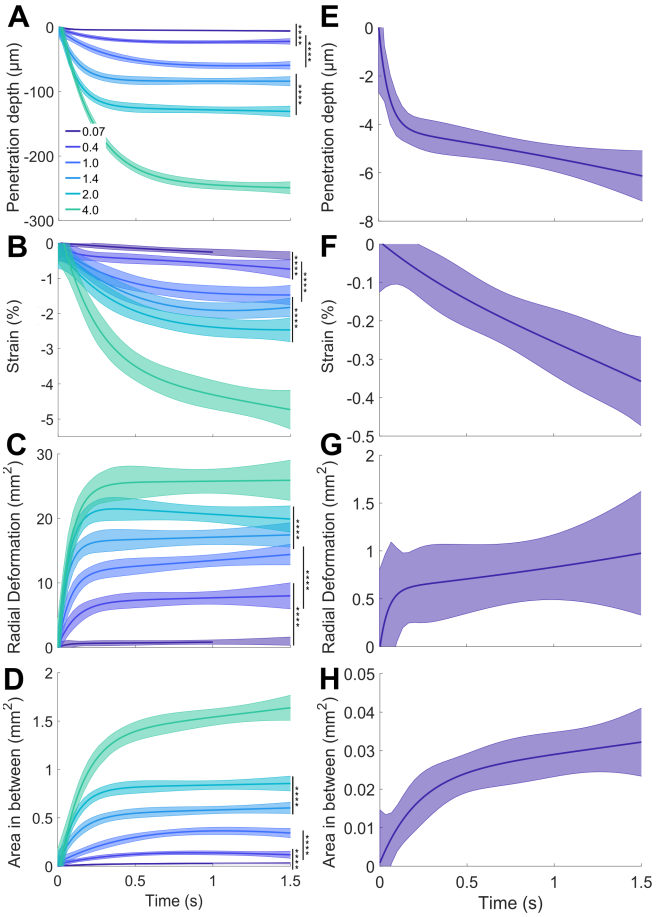

Figure 4. Skin deformation metrics in response to von Frey monofilaments (force range: 0.07 – 4.0 g). (A)-(D) Experimental data from all participants and trials. Solid curves indicate an exponential fit to the raw data. Shaded regions represent the upper and lower 95% confidence intervals of the fit and ****p < 0.0001, by the two-sample t-test. (E)-(H) Plots showing metrics for only the 0.07 g monofilament with adjusted y-axis scale to illustrate DIC tracking of deformation at the micrometer level.

paradigm [12] – was encountered at 0.4 g across both no paint and paint conditions, with the 0.07 g monofilament just beneath this threshold. These findings align with prior studies with greater numbers of participants, with a force detection threshold similar with Semmes-Weinstein monofilaments of 0.07 g used at the forehead and palm, and 0.4 g at the arm [12]. With respect to discrimination thresholds (Fig. 5F), participants could discriminate only the smallest pair (0.07, 0.4 g) at levels of 75% correct. A decline in discriminability was observed with higher monofilament force. That is, while the two indiscriminable pairs were separated by 0.6 g force, the (1.4, 2.0 g) pair yielded worse performance, i.e., near chance, as opposed to the (0.4, 1.0 g) pair.

Exploration into the effects of the application of the paint layer on the skin surface revealed no systematic impact on perceptual response, Fig. 5A. We would like to note, however, that these findings are restricted to the range of monofilaments used in this study (0.02 – 4.0 g) and a relatively modest cohort of participants (N=5).

C. Comparison of skin deformation and psychophysics

Psychophysical evaluation indicated an absolute detection threshold at the 0.4 g monofilament (Fig. 5A). Prior literature has shown that this threshold lies near either the 0.07 or 0.4 g monofilament, depending on exact brand of monofilament and body site [12]. Our imaging yields non-zero skin deformation with both monofilaments. In particular, for the 0.07 g monofilament, penetration depth was 6.1 µm, strain was 0.34%, radial deformation was 0.96 mm^2, and area between 2D cross-sections was 0.03 mm^2 (Figs. 4E-H). The correlation between the four biomechanical variables and perceptual performance, unique to each participant, was quantified with the psychometric function fitted by a beta-binomial model [19], Figs. 5B-E. All four derived metrics follow a sigmoidal curve, typical of such data, depicting an increase in absolute detection with skin deformation. For example, 80% threshold is reached at 11.48 µm penetration depth, 0.22% strain, 2.84 mm^2 radial deformation, and 0.05 mm^2 area between 2D cross-sections. Investigating these relationships provides further insight into direct ties between levels of skin deformation and perception.

With respect to discrimination thresholds, the psychophysical evaluation shows only the smallest pair (0.07, 0.4 g) were discriminable (Fig. 5F). Likewise, with the four derived skin deformation metrics, this pair of monofilaments produces the largest differences (Fig. 4A-D). In particular, the 0.07 g monofilament had a penetration depth of 6.1 µm, while the 0.4 g monofilament had a penetration depth of 23.4 µm ($t(383) = 20.32$, $p < 0.0001$). Similarly, strain reached 0.34% for the 0.07 g monofilament, and 0.72% for the 0.4 g monofilament ($t(383) = 8.04$, $p < 0.0001$). Radial deformation increased 0.96 to 7.97 mm^2 ($t(413) = -17.80$, $p < 0.0001$), and area between 2D cross-sections increased 0.03 to 0.14 mm^2 ($t(383) = -17.33$, $p < 0.0001$).

Moreover, as shown in Figs. 5G-J, the percent integral difference per discrimination pair was calculated over time for the four derived metrics. We observe correspondence in the relative ordering of these pairs with the ordering of percentage correct in the psychophysical experiment (Fig. 5F), depicting larger differences at lower force (0.07, 0.4 g) as compared to higher force (1.4, 2.0 g).

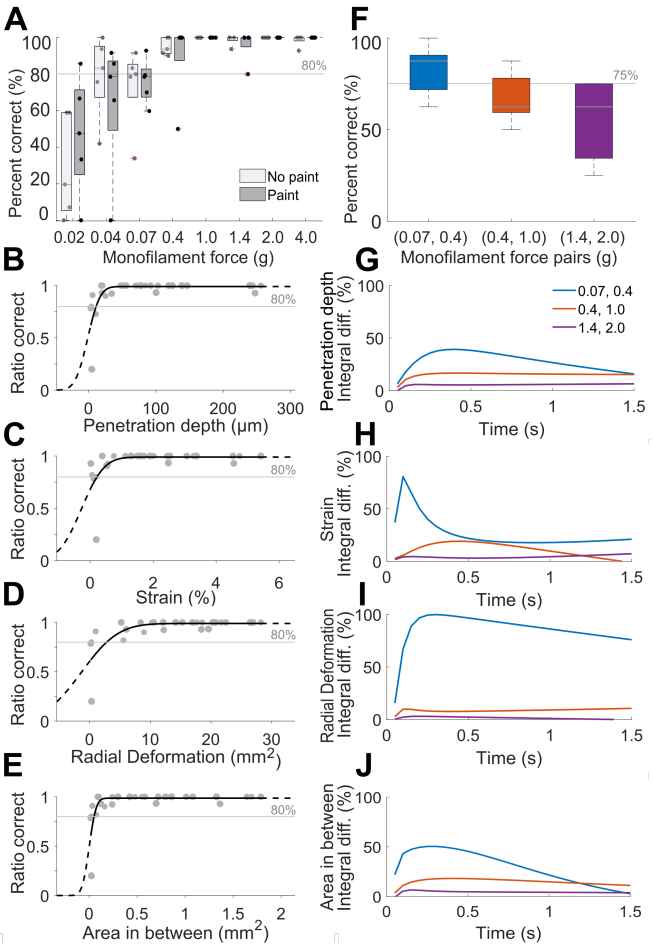

Figure 5. Results of psychophysical evaluation of absolute detection and discrimination threshold. (A) Absolute detection results showing average percent correct of trials for all participants in ascending and descending order in box whisker plots, where experiments conducted with and without paint on the finger pad skin yielded a negligible difference. (B)-(E) Psychometric plots depicting individual subject skin deformation of the five participants linked to their psychophysical results. (F) Discrimination results for pairs of monofilaments. For (A) and (F), N=5 participants, error bars in (F) show standard deviation. (G)-(J) Percent integral difference per metric between the three monofilaments pairs. Their ordering indicates a greater normalized difference for the smallest monofilament pair (0.07, 0.4 g) as compared to the other two pair, aligning with psychophysical results in panel (F).

IV. Discussion

This work adopts an imaging approach using digital image correlation with standard high-resolution cameras to evaluate 3D mechanical states of deformation at the skin surface, upon indentation by monofilaments. Von Frey monofilaments are an important tool in the clinical assessment of neuropathic impairment. The empirical quantification of skin states at perceptual thresholds may ultimately aid clinicians in better understanding the neurological origins of particular sensory impairments. The results indicate that this approach indeed achieves sufficient resolution and range to capture distinct states of skin deformation at just noticeable thresholds of absolute detection and discrimination.

In our psychophysical evaluation of absolute detection, in agreement with prior studies with greater numbers of

participants [1], [12], we find the perceptual threshold in the distal skin of the finger pad lies between 0.07 and 0.4 g. In comparison, in terms of resolution, the imaging approach measures non-zero skin deformation for the 0.07 g stimulus at 6.1 μm penetration depth, 0.34% strain, 0.96 mm^2 radial deformation, and 0.03 mm^2 of area between 2D cross-sections, demonstrating the ability to quantify small deformation at the perceptual threshold. Moreover, this penetration depth aligns with studies showing embossed dots as small at 8 and 1-3 μm elicit responses from slowly and rapidly adapting afferents, respectively. Moving forward, additional work is needed to evaluate the capability of the imaging below forces of 0.07 g, as von Frey monofilaments continue to 0.008 g.

Across the biomechanical metrics, the results depict clear separation in states of skin deformation between von Frey monofilaments, likely to drive responses of peripheral afferents. For example, we report that the 4.0 g case penetrates 62% more deeply than the 2.0 g case (248.9 μm vs. 130.6 μm) with similar differences in strain (4.69% vs. 2.46%), Fig. 4A, B. Although prior works show that stimulus force relates to perception [1], [12], the differences in penetration depth and strain begin to address a key missing step, i.e., how the skin deforms in response to the stimulus. Additional biomechanical metrics, such as patterns of radial deformation, may drive mechanisms of neural coding by primary afferents as well. Overall, we know that afferent firing frequency increases with force, receptive field sizes increase with force to a maximum, and multiple receptive fields overlap each other to inform a population response [15]. In comparison, in Fig. 4C we observe clearly differentiable increases in penetration depth over the time of the indentation ramp, areas of radial deformation (1.0 g case, 14.3 mm^2) of about the same magnitude as maximum receptive field sizes for SAI (12.6 mm^2) and RA (11.0 mm^2) afferents in the hand [20], and smaller areas of deformation (0.07 g case) that grow from about 0.25 mm^2 to a size of 0.96 mm^2. One would expect such patterns of skin deformation to evoke informative responses from a population of afferents.

In the discrimination tasks, participants were better at distinguishing the lower force pair of monofilaments (0.07, 0.4 g), Fig. 5F. We hypothesize that improved performance for this pair is due to participants only detecting the 0.4 g monofilament with high confidence, because Fig. 5A shows that the 0.07 g case lies very near the threshold of absolute detection. Comparatively, with the higher force pairs of monofilaments (0.4, 1.0 g) and (1.4, 2.0 g), participants can detect each monofilament. They therefore are likely to discriminate within a pair based on changes in patterns of skin deformation. Indeed, Figs. 5G-J depict higher relative changes in all biomechanical metrics for the middle force pair (0.4, 1.0 g) compared to the highest force pair (1.4, 2.0 g). For example, we measure integral differences of 16.5% penetration depth and 18.9% strain for the middle force pair (0.4, 1.0 g), while only 5.3% penetration depth and 6.8% strain for the largest force pair (1.4, 2.0 g). The larger relative changes in skin states within a monofilament pair may improve discriminative performance.

REFERENCES

[1] J. A. Bell-Krotoski, E. E. Fess, J. H. Figarola, and D. Hiltz, "Threshold Detection and Semmes-Weinstein Monofilaments," *J. Hand Ther.*, vol. 8, no. 2, pp. 155–162, Apr. 1995.

[2] J. Bell-Krotoski, S. Weinstein, and C. Weinstein, "Testing sensibility, including touch-pressure, two-point discrimination, point localization, and vibration," *J. Hand Ther. Off. J. Am. Soc. Hand Ther.*, vol. 6, no. 2, pp. 114–123, Jun. 1993.

[3] Y. Wang, Y. Baba, E. A. Lumpkin, and G. J. Gerling, "Computational modeling indicates that surface pressure can be reliably conveyed to tactile receptors even amidst changes in skin mechanics," *J. Neurophysiol.*, vol. 116, no. 1, Art. no. 1, Jul. 2016.

[4] B. P. Delhaye, E. Jarocka, A. Barrea, J.-L. Thonnard, B. Edin, and P. Lefèvre, "High-resolution imaging of skin deformation shows that afferents from human fingertips signal slip onset," *eLife*, vol. 10, p. e64679, Apr. 2021.

[5] B. Delhaye, A. Barrea, B. B. Edin, P. Lefèvre, and J.-L. Thonnard, "Surface strain measurements of fingertip skin under shearing," *J. R. Soc. Interface*, vol. 13, no. 115, Art. no. 115, Feb. 2016.

[6] S. C. Hauser and G. J. Gerling, "Force-rate Cues Reduce Object Deformation Necessary to Discriminate Compliances Harder than the Skin," *IEEE Trans. Haptics*, vol. 11, no. 2, pp. 232–240, 2018.

[7] X. Liu, R. Maiti, Z. H. Lu, M. J. Carré, S. J. Matcher, and R. Lewis, "New Non-invasive Techniques to Quantify Skin Surface Strain and Sub-surface Layer Deformation of Finger-pad during Sliding," *Biotribology*, vol. 12, pp. 52–58, Dec. 2017.

[8] R. Maiti *et al.*, "In vivo measurement of skin surface strain and sub-surface layer deformation induced by natural tissue stretching," *J. Mech. Behav. Biomed. Mater.*, vol. 62, pp. 556–569, Sep. 2016,

[9] Z. S. Lee, R. Maiti, M. J. Carré, and R. Lewis, "Morphology of a human finger pad during sliding against a grooved plate: A pilot study," *Biotribology*, vol. 21, p. 100114, Mar. 2020.

[10] Z. Xu, J. D. Cruz, C. Fthenakis, and C. Saliou, "A novel method to measure skin mechanical properties with three-dimensional digital image correlation," *Skin Res. Technol.*, vol. 25, no. 1, pp. 60–67, 2019.

[11] B. Li, S. Hauser, and G. J. Gerling, "Identifying 3-D spatiotemporal skin deformation cues evoked in interacting with compliant elastic surfaces," in *2020 IEEE Haptics Symposium (HAPTICS)*, Mar. 2020, pp. 35–40.

[12] R. Ackerley, I. Carlsson, H. Wester, H. Olausson, and H. Backlund Wasling, "Touch perceptions across skin sites: differences between sensitivity, direction discrimination and pleasantness," *Front. Behav. Neurosci.*, vol. 8, p. 54, Feb. 2014.

[13] J. R. Deuis, L. S. Dvorakova, and I. Vetter, "Methods Used to Evaluate Pain Behaviors in Rodents," *Front. Mol. Neurosci.*, vol. 10, p. 284, Sep. 2017.

[14] C. Xu, Y. Wang, and G. J. Gerling, "An elasticity-curvature illusion decouples cutaneous and proprioceptive cues in active exploration of soft objects," *PLoS Comput. Biol.*, vol. 17, no. 3, p. e1008848, Mar. 2021.

[15] R. S. Johansson, "Tactile sensibility in the human hand: receptive field characteristics of mechanoreceptive units in the glabrous skin area.," *J. Physiol.*, vol. 281, no. 1, pp. 101–125, 1978.

[16] D. Solav, K. M. Moerman, A. M. Jaeger, K. Genovese, and H. M. Herr, "MultiDIC: An Open-Source Toolbox for Multi-View 3D Digital Image Correlation," *IEEE Access*, vol. 6, pp. 30520–30535, 2018.

[17] J. Blaber, B. Adair, and A. Antoniou, "Ncorr: Open-Source 2D Digital Image Correlation Matlab Software," *Exp. Mech.*, vol. 55, no. 6, pp. 1105–1122, Jul. 2015.

[18] O. Levano Blanch, D. Lunt, G. J. Baxter, and M. Jackson, "Deformation Behaviour of a FAST Diffusion Bond Processed from Dissimilar Titanium Alloy Powders," *Metall. Mater. Trans. A*, vol. 52, no. 7, pp. 3064–3082, Jul. 2021.

[19] H. H. Schütt, S. Harmeling, J. H. Macke, and F. A. Wichmann, "Painfree and accurate Bayesian estimation of psychometric functions for (potentially) overdispersed data," *Vision Res.*, vol. 122, pp. 105–123, May 2016.

[20] R. S. Johansson and Å. B. Vallbo, "Spatial properties of the population of mechanoreceptive units in the glabrous skin of the human hand," *Brain Res.*, vol. 184, no. 2, pp. 353–366, Feb. 1980.